INSTITUTE OF PLASMA PHYSICS

NAGOYA UNIVERSITY

RESEARCH REPORT

NAGOYA, JAPAN

New Lens System Using Toroidal Magnetic Field for Intense Ion Beam

Akihiro MOHRI, Kazunari IKUTA

and

Junji FUJITA

IPPJ-264 November 1976

Further communication about this report is to be sent to the Research Information Center, Institute of Plasma Physics, Nagoya University, Nagoya, Japan.

Permanent address : Institute of Plasma Physics,
Nagoya University, Nagoya, Japan.

Abstract

The use of toroidal magnetic field as a lens system is proposed for producing intense ion beam. The characteristics of the lens system are obtained both analytically and numerically. Some examples of ray-trajectories are presented for different focal lengths. The system is applicable to neutral beam injection heating and micro-pellet i implosion for nuclear fusion, and to the other fields such as ion beam X-ray lasers.

1. Introduction

There is an increased interest to have intense ion beam in the field of nuclear fusion. Efforts have extensively been made to increase the extractable current density of the beam source,[1] while very few attempts have been seen to intensify the density by converging the extracted beam. Conventional magnetic lens, which uses converging lines of force, is based on the principle of energy conservation and the adiabatic invariant in the static magnetic field. However, this system of converging lines of force has two fatal disadvantages in application: i) Intensifying ratio of beam particle is in proportion to the ratio of the field strength at the exit to the one at the entrance. The ratio is at most of the order of 10^2 from the technical reason. ii) The lens is apt to perturb the magnetic confinement system of plasma because the magnetic flux diverges out of the lens system.

We here consider a magnetic lens system which gives practically no magnetic perturbation to the confinement systems. An axisymmetric toroidal magnetic field can be used for the purpose since the toroidal lines of force close themselves in a finite volume. This lens has, in principle, no limitation in the intensification of the beam particle density. Section 2 is devoted to analyses of lens characteristics. In Section 3 possible applications of the lens system to nuclear fusion and the others are illustrated.

2. Principle of the Magnetic Lens

2.1 Formulation of beam trajectories

The magnetic lens being discussed here uses the deflection of incident ions in a toroidal magnetic field. After travelling in free space, charged particles enter the region of the magnetic field in which the particles change their direction of velocity by a pertinent amount, and then the particles leave the magnetic field region directing towards the focusing point. Figure 1 shows an example of the trajectories. The toroidal magnetic field, therefore, should be localized in the hatched region in the figure. We shall find this boundary of the field which depends on both the field strength and the charge to mass ratio of the particles.

We use cylindrical coordinates (r, θ, z). The z-axis is chosen to be the major axis of a toroidal field B_θ, as is depicted in Fig.1. The toroidal field is present in a bounded region between $z = 0$ plane and another boundary which is to be solved. Ions with the velocity $\vec{v}$ enter the field region at $z = 0$ in parallel to the z-axis at the time $t = 0$. The equation of motion for the ions is

$$m \frac{d\vec{v}}{dt} = e\vec{v} \times \vec{B} , \qquad (1)$$

where m and e are the mass and the charge of the ion, respectively. As $B_\theta = B(a/r)$, Eq.(1) is reduced to

$$\frac{dv_r}{dt} = -\Omega \frac{a}{r} v_z ,$$

$$\frac{dv_z}{dt} = \Omega \frac{a}{r} v_r \ , \qquad (1)'$$

where a is the radius of lens aperture and $\Omega = eB/m$. Under the initial conditions at $t = 0$,

$$r = r_s, \quad z = 0, \quad \frac{dr}{dt} = 0 \quad \text{and} \quad \frac{dz}{dt} = v \ ,$$

the components of velocity are found to be

$$\frac{dr}{dt} = -v[1 - \{1 + \frac{\Omega a}{v} \ln(\frac{r}{r_s})\}^2]^{1/2} \mathrm{Sign}(\Omega) \ , \qquad (2)$$

and

$$\frac{dz}{dt} = v + \Omega a \ell n(\frac{r}{r_s}) \ . \qquad (3)$$

Hereafter we shall use the following normalizations

$$R = r/a \ , \qquad Z = z/a \ ,$$

and the parameter

$$\xi = \Omega a/v \ .$$

Defining a function

$$g(x, \xi) = \frac{[1 - (1 + \xi \ln x)^2]^{1/2}}{1 + \xi \ln x} \ , \qquad (4)$$

we have from Eqs.(2) and (3)

$$\frac{dR}{dZ} = -g(\frac{R}{R_s}, \xi) \cdot \mathrm{Sign}(\Omega) \ , \qquad (5)$$

which shows the direction of the ion motion. Then, the trajectory of the ion motion is expressed by

$$Z = -G(R/R_s, \xi)\cdot \mathrm{Sign}(\Omega) \ , \tag{6}$$

where

$$G(R/R_s, \xi) = \int_{R_s}^{R} \frac{dR}{g(R/R_s, \xi)} \ .$$

At the exit boundary of the magnetic field where $R = R_p$ and $Z = Z_p$, the ion should move straight towards the focusing point ($R = 0$, $Z = D$). Thus we can have a simultaneous equation to find the exit boundary (R_p, Z_p) as

$$\begin{aligned} g(R_p/R_s, \xi)\cdot \mathrm{Sign}(\Omega) &= \frac{R_p}{D - Z_p} \ , \\ \text{and} \qquad & \qquad (7) \\ Z_p &= -G(R_p/R_s, \xi)\cdot \mathrm{Sign}(\Omega) \end{aligned}$$

The boundary surface of the magnetic region on the exit side can be determined as a contour of (R_p, Z_p) with respect to R_s.

The parameter $\xi = \Omega a/v$ is an essential one for this magnetic lens. For example ξ affects the focal length. Let us consider a lens to focus the ions which enter the lens at the point P_s ($R_s = 1$, $Z = 0$) and depart at the exit P_d ($R = R_{pd}$, $Z = D$) with zero axial velocity. Then from Eq.(7),

$$R_{pd} = e^{-1/\xi} \ .$$

Typical relations between R_{pd} and ξ are shown below.

$$R_{pd} \to 1 \qquad \text{for} \qquad \xi \to \infty$$

$$R_{pd} = 1/2 \qquad \text{for} \qquad \xi = 1.44$$

$$R_{pd} = 1/e \qquad \text{for} \qquad \xi = 1$$

$$R_{pd} \to 0 \qquad \text{for} \qquad \xi \to 0$$

These relations suggest that large ξ corresponds to short focal lens, whereas small ξ to long focal lens.

2.2 Approximate approach

Numerical methods have to be used to solve Eq.(7) in general. However, we can approximately solve it in the case of small ξ (i.e., long focal length). In this case, the deflection of the ion beam inside the magnetic lens is small so that we can use a small quantity defined by

$$\gamma_p = \frac{R_p - R_s}{R_s} .$$

Equation (7) is now approximated as

$$\begin{aligned} \sqrt{-2\xi\gamma_p}\cdot \mathrm{Sign}(\Omega) &= R_p/(D - Z_p) \\ (1/\xi)\sqrt{-2\xi\gamma_p}\cdot \mathrm{Sign}(\Omega) &= Z_p/R_p \end{aligned} \qquad (8)$$

to the order of $\gamma_p^{1/2}$. Therefore, we have

$$R_p \simeq \sqrt{\xi D Z_p} \ , \tag{9}$$

which gives the exit boundary of the lens. The surface is parabolic as is shown in Fig.2. The relation (9) is valid to both the convex lens ($\xi > 0$, $D > 0$) and the concave one ($\xi < 0$, $D < 0$).

In the above discussion we have considered the mono-energetic ion beam. We shall see the effect of the velocity spread of ions from a given value. Differentiation of Eq.(9) for constant R_p and Z_p leads to the relation

$$dD = \left(\frac{v_o}{\Omega a}\right)\left(\frac{R_p^2}{z_p}\right)\left(\frac{dv}{v_o}\right) = D\left(\frac{dv}{v_o}\right) \ ,$$

where v_o is the most probable velocity of ions. The aberration due to the broadening of the velocity distribution becomes larger as going outwards from the axis and also as the focal length increases. These characteristics are akin to usual optical lens. In order to concentrate the energy of ion beam with some velocity spread on a very small locus we must use the magnetic lens with short focal length (i.e., large ξ).

2.3 Numerical results

The accurate exit boundary of the magnetic lens can be determined numerically either by solving Eq.(7) for (R_p, Z_p) or by finding the positions where the travelling ions inside

the lens direct their velocities at the focal point. In this section the boundary surfaces obtained by the latter method are presented for different values of the relative aperture 1/D and the parameter $\xi = \Omega a/v$.

Figure 3 shows boundaries of long focal length where ξ and 1/D are both small. The exit boundary surfaces are nearly parabolic as discussed in the previous section. The trajectories of the beam ions are also shown.

The shape of the exit boundary largely deviates from the parabolic one in the case of short focal length where ξ is large and D is small. Figure 4 shows the change of the shape with the parameter ξ for D = 1.0. When ξ is fairly large (Fig.4(a)), the ions moving inside the lens are easily deflected and, as a result, required depth of the lens becomes small compared with that for smaller ξ. As ξ is decreased, the exit boundary surface should deform its shape from parabolic one as is seen in Figs.4(b)-(d).

Another example of short focal length is presented in Fig.5(a) where D = 0.5. When the incident flux density of ion beam is uniform, the angular distribution around the focal point can not be isotropic as is shown in Fig.5(b). If further isotropy is necessary according to the purpose of use, some expedients have to be adopted.

2.4 Neutralization of space charge

If the space charge of beam ions is not neutralized, the resultant electric field and magnetic field would affect the orbits of ions. The effect of the non-neutrality might

become significantly severe near the focal point where the density of ions is highest. However, the neutralization of the space charge is easily accomplished by seeding electrons as is schematically depicted in Fig.6. Electron emitters installed inside the magnetic lens eject electrons parallel to the toroidal magnetic field, and the electrons drift towards the upper stream of the ion beam. The magnetic lens is thereby filled with an electron cloud of the density which is enough to neutralize the space charge inside the lens. Besides, electrons supplied by emitters on the outer side of the lens are dragged by the beam ions and follow the motion of ions. Therefore, neither electric field nor magnetic field appear during the focusing of the ion beam.

3. Applications of the Lens

3.1 Generation of neutral beam of high current density

Neutral beam injection into a confined plasma will be a powerful means to raise the temperature up to a sufficient one for nuclear fusion.[2] Fusion reactors using D-T reactions should be equipped with thick shielding walls for neutrons and radiations which come out of the central burning plasma.[3] External magnetic coils for plasma confinement occupy the large part of the space outside the walls. Therefore, the channel which connects the ion beam source to the plasma is favoured to be as narrow as possible. This means that injection heating cannot be attained without the development of neutral beams with high current density.

However, the extractable current density of an ion beam

from plasma is limited by the Child-Langmuir's law. The magnetic lens proposed here can solve this difficult problem.

Figure 7 shows a conceptional drawing of the lens system to have neutral beams of high current density. Ion beams extracted in the usual manner are introduced into the convex lens. The beam is converged by a convex lens and electrostatically neutralized. During the focusing the flux density of the ion beam increases. The beam is again expanded by a concave lens and finally a parallel beam of high flux density is formed. A charge exchanger, which is set on the downstream, converts the ion beam to a neutral beam. Impurity ions in the beam are easily taken away during the passage through the system since they suffer different deflections inside the lens. Thus, a pure neutral beam of high flux density can be obtained.

3.2 Micro-pellet fusion by ion beams

Micro-implosion of solid or shelled gas pellets by high power laser or by relativistic electron beam pinch is now under extensive investigations aiming pulsed release of fusion power. In a similar way the use of high power ion beam may be considered. Generation of pulsed ion beams of high particle energy is now being developed.[4] In quite near future a single ion beam at the output level of terawatt will become usable. However, the self-pinch of ion beams on a small pellet is difficult in principle because of the large mass of ions. There should be other methods to focus ion beams on a small point. The magnetic lens for ion beam

will give a solution of the problem. It should be stressed that the stopping range of an energetic ion in solid material is much shorter than that of an electron. Efficient super-compression of a pellet is expected by the use of the ion beam focusing.

Figure 8 shows a schematic explanation of the micro-implosion of a pellet by focusing ion beams. Two magnetic lenses are faced each other and the pellet is laid at the centre of the system. The ion beams coming down from both the sides are focused on the pellet by the magnetic lens. A system of multichannel ion beams is useful to adjust the timing of the irradiation and to improve the uniformity of the power on the target.

3.3 Intense ion beam for X-ray lasers

The use of intense ion beam has been proposed for the purpose of realizing X-ray lasers, based on the fact that the cross section for the collision processes causing the population inversion is much larger for the case of ion-neutral or ion-ion interactions than the one for electron-neutral or electron-ion interactions.

Up to now, however, nobody has been successful in achieving X-ray lasers because of the difficulty to produce ion beams of sufficient intensity.

The toroidal magnetic lens here proposed has a great advantage that the axis is, in principle, completely open for the other uses, for example, letting the light beam pass through. This feature is exactly what is needed for realiz-

ing the ion beam lasers. The system proposed is schematically shown in Fig.9, where the similar ion beam system described in Sec.3.1 is adopted.

4. Conclusive Remarks

A lens system using toroidal magnetic field has been proposed and its several applications have been considered such as neutral beam injection heating, micro-pellet implosion and ion beam X-ray lasers. In this paper, the sharp boundaries of the toroidal magnetic field have been assumed so as to demonstrate the lens action of the field. Practically, ion beams should pass through the interspace between the current carrying conductors which produce the toroidal field. In this case the field is not sharply bounded in the strict sense, so that the corrugation of the field should be taken into account when the lens system is designed.

Instead of the toroidal field, the similar lens action can be achieved with a system of feromagnets which are periodically arranged in the toroidal direction. Only a sector of the system is also used depending on purposes.

References

1) O.B.Morgan, G.G.Kelley and R.C.Davis: Rev.Sci.Instr. 38(1967)467.

2) T.H.Stix: Plasma Phys. 14(1972)367.

3) D.J.Rose: Nuclear Fusion 9(1969)183.

4) S.Humphries, J.J.Lee and R.N.Sudan: Appl.Phys.Lett. 25(1974)20; K.Ikuta, A.Mohri and M.Masuzaki: Japan. J.Appl.Phys. 14(1975)1569; R.N.Sudan and R.V.Lovelace: Phys.Rev.Lett. 31(1973)1174.

5) T.Suzuki and W.Shearer-Izumi: BUTSURI(in Japanese) 31(1976)640.

Figure Captions

Fig.1. Principle of the toroidal magnetic lens.

Fig.2. Converging (convex) and diverging (concave) magnetic lenses.

Fig.3. Trajectories of ions for the toroidal magnetic lens with long focal length.

Fig.4. Change of the exit boundary of the lens with the parameter ξ for the fixed focal length D = 1.0. Trajectories of ions are also shown.

Fig.5. Typical example in the case of short focal length. (a) Beam trajectories, (b) angular distribution of the flux density around the focal point.

Fig.6. Method to cancel the space charge of ion beam.

Fig.7. Lens system to generate intense neutral beam. IS: ion source, CVL: convex lens, CCL: concave lens, BC: burial chamber for high Z impurities, CN: charge exchange neutralizer, F: common focal point.

Fig.8. Conceptual drawing of the micro-pellet implosion system with double toroidal magnetic lenses.

Fig.9. Conceptual drawing of the ion beam X-ray laser. IS: ion beam source, CVL: convex lens, S: metal vapour source, C: condenser.

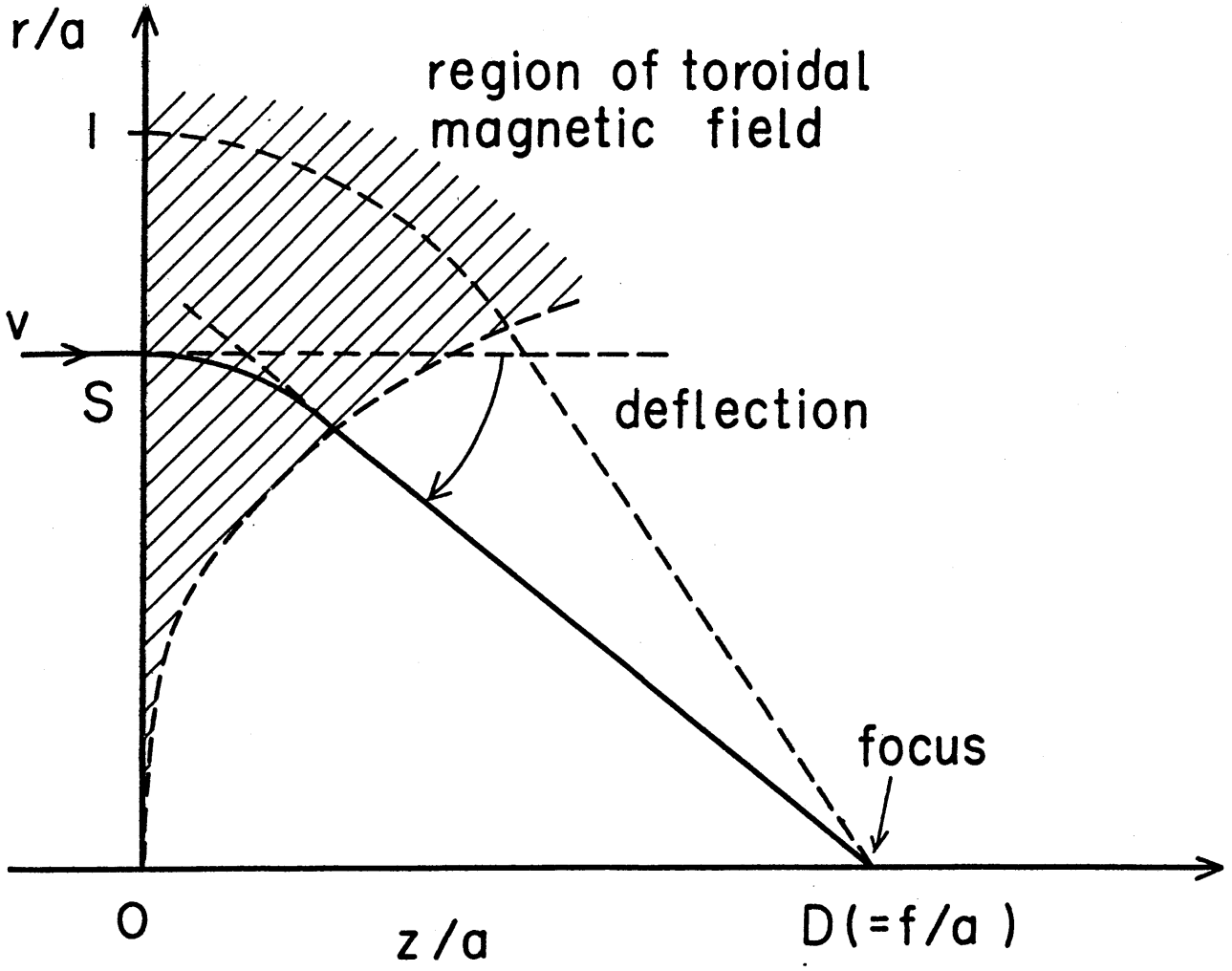
r/a
region of toroidal
magnetic field
1
v
S
deflection
focus
0
z/a
D(=f/a)

FIG. 1

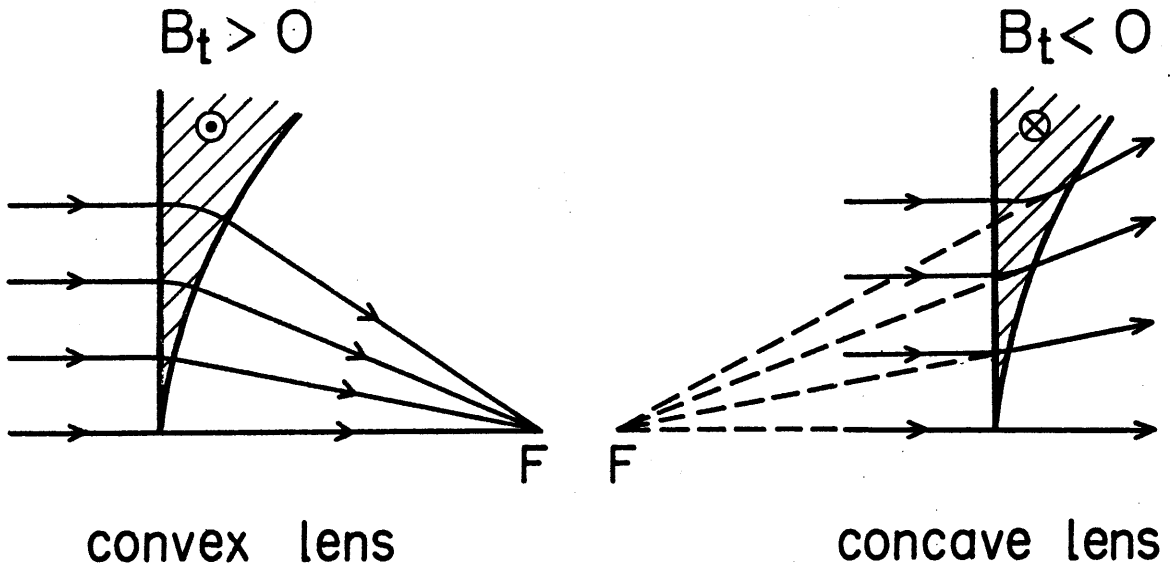

FIG. 2

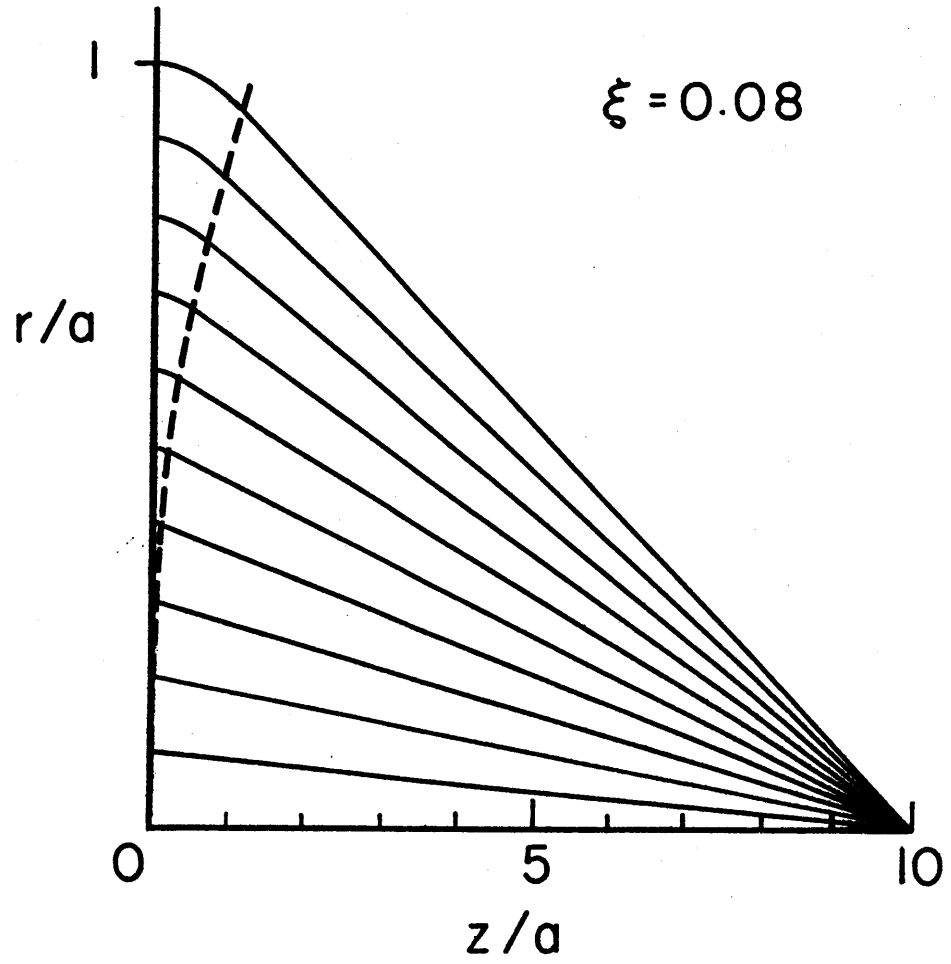

FIG. 3

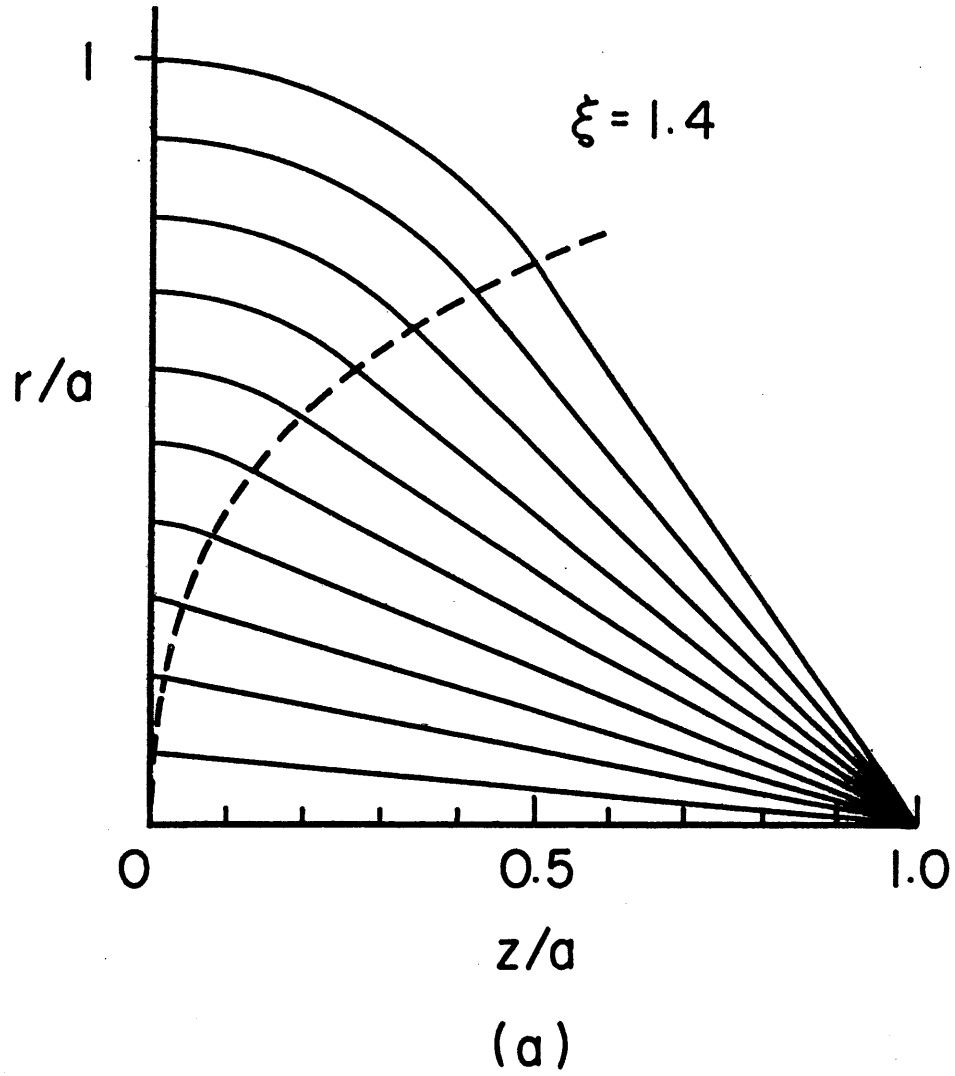

FIG. 4(A)

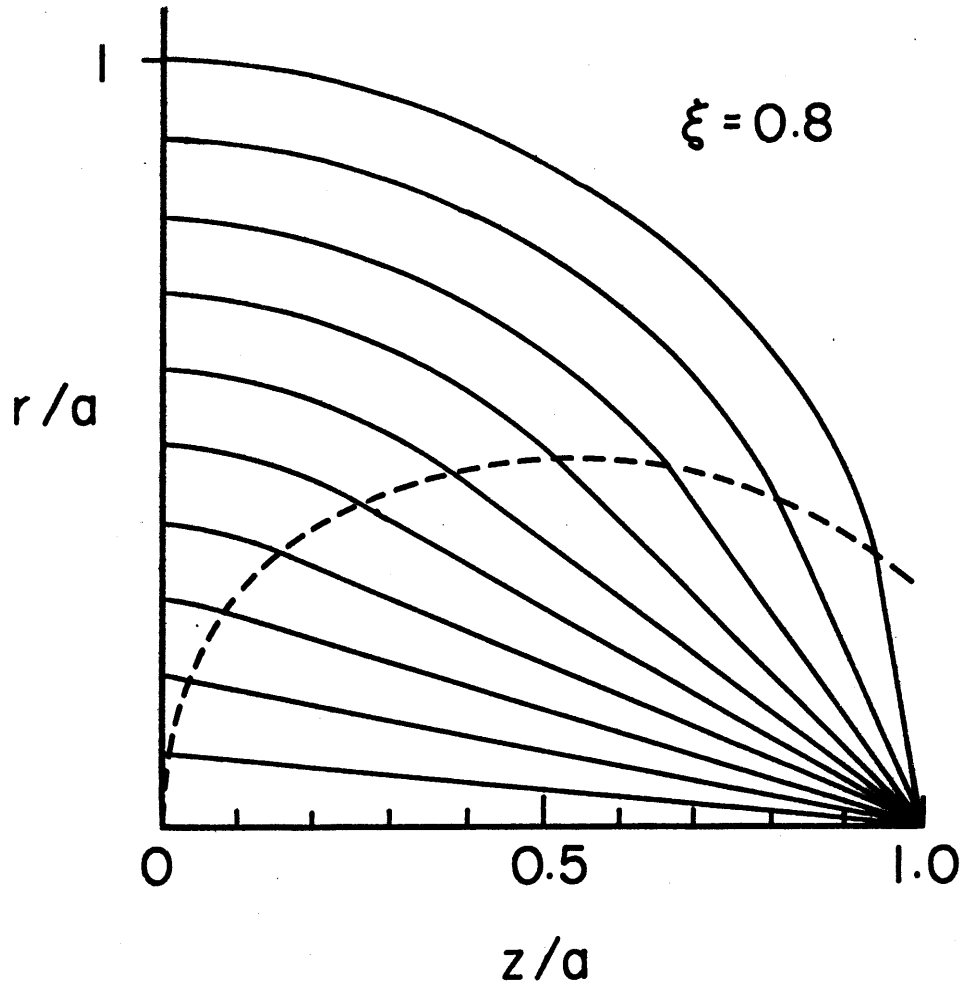

(b)

FIG. 4(B)

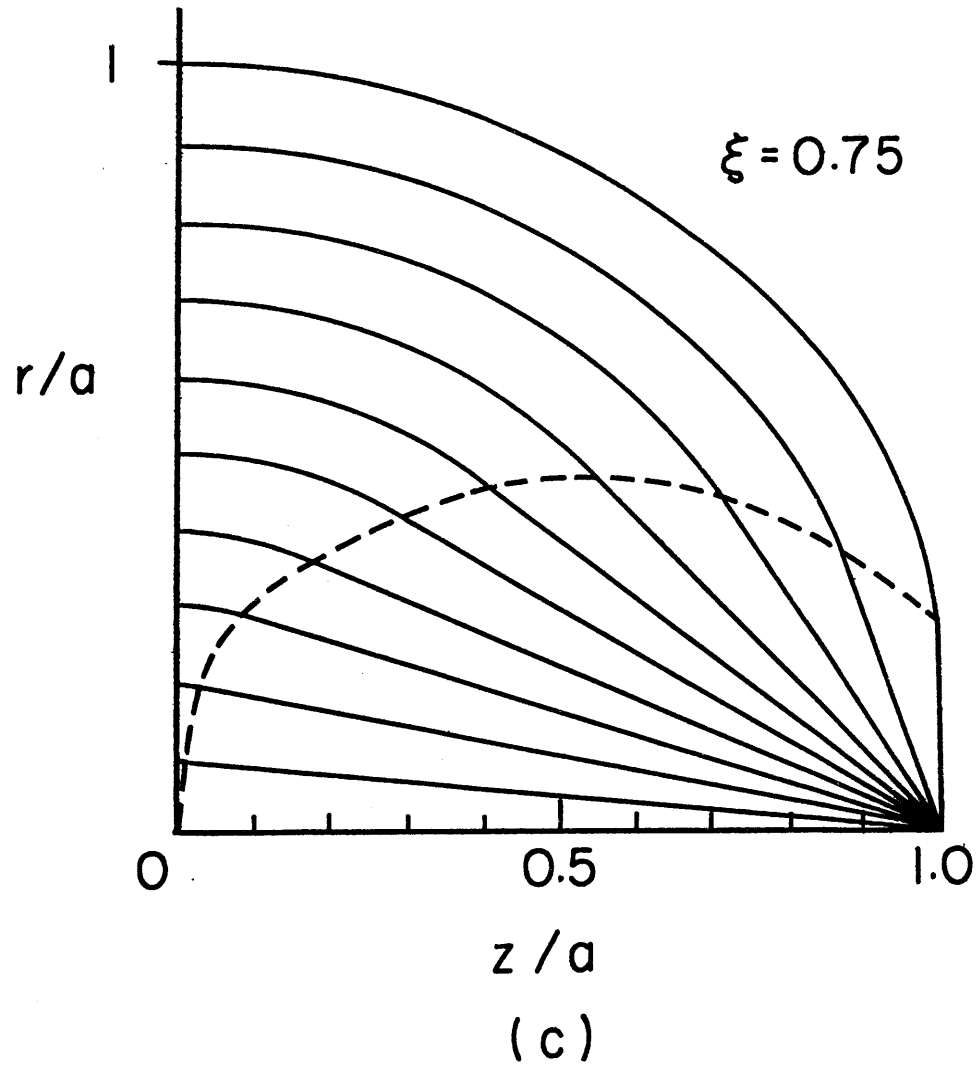

FIG. 4(c)

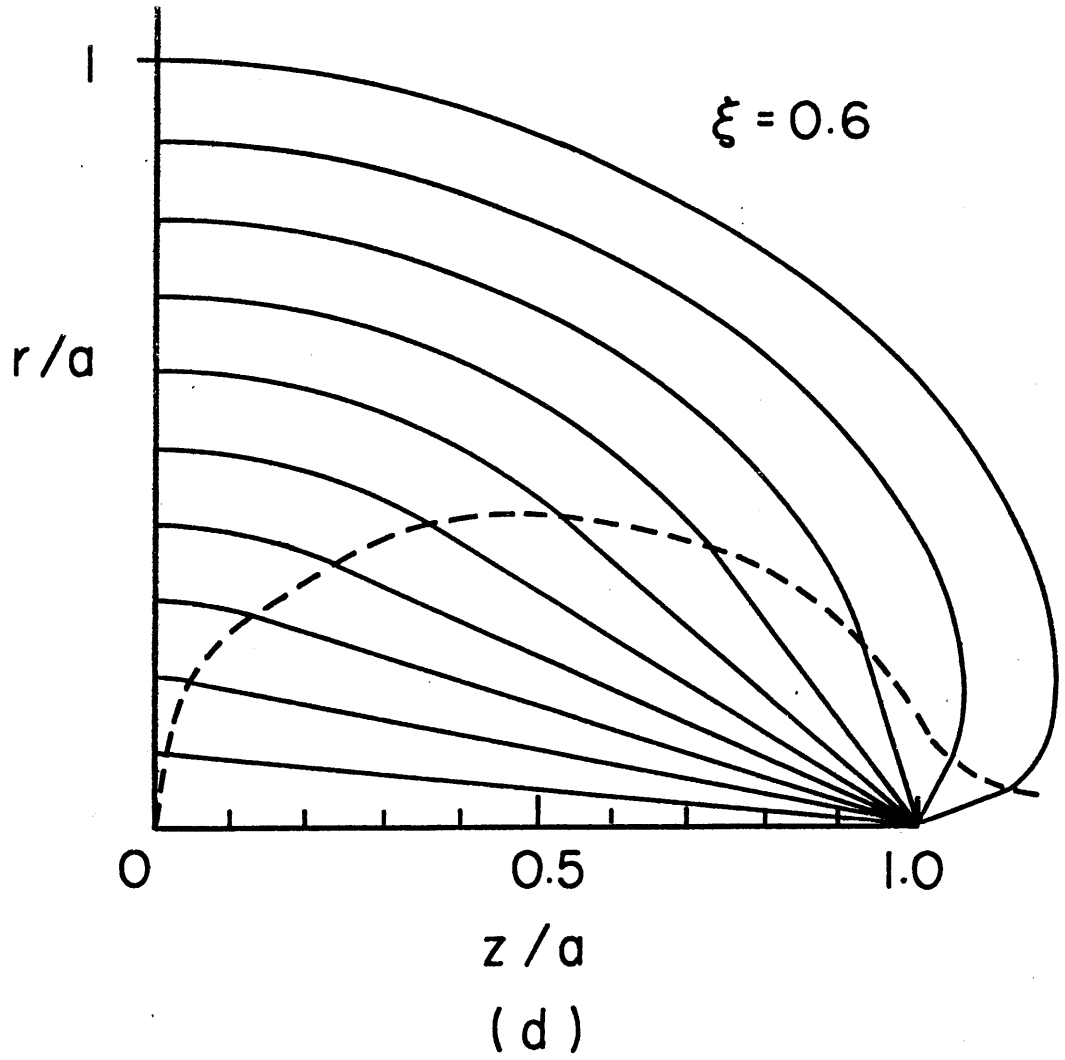

FIG. 4(D)

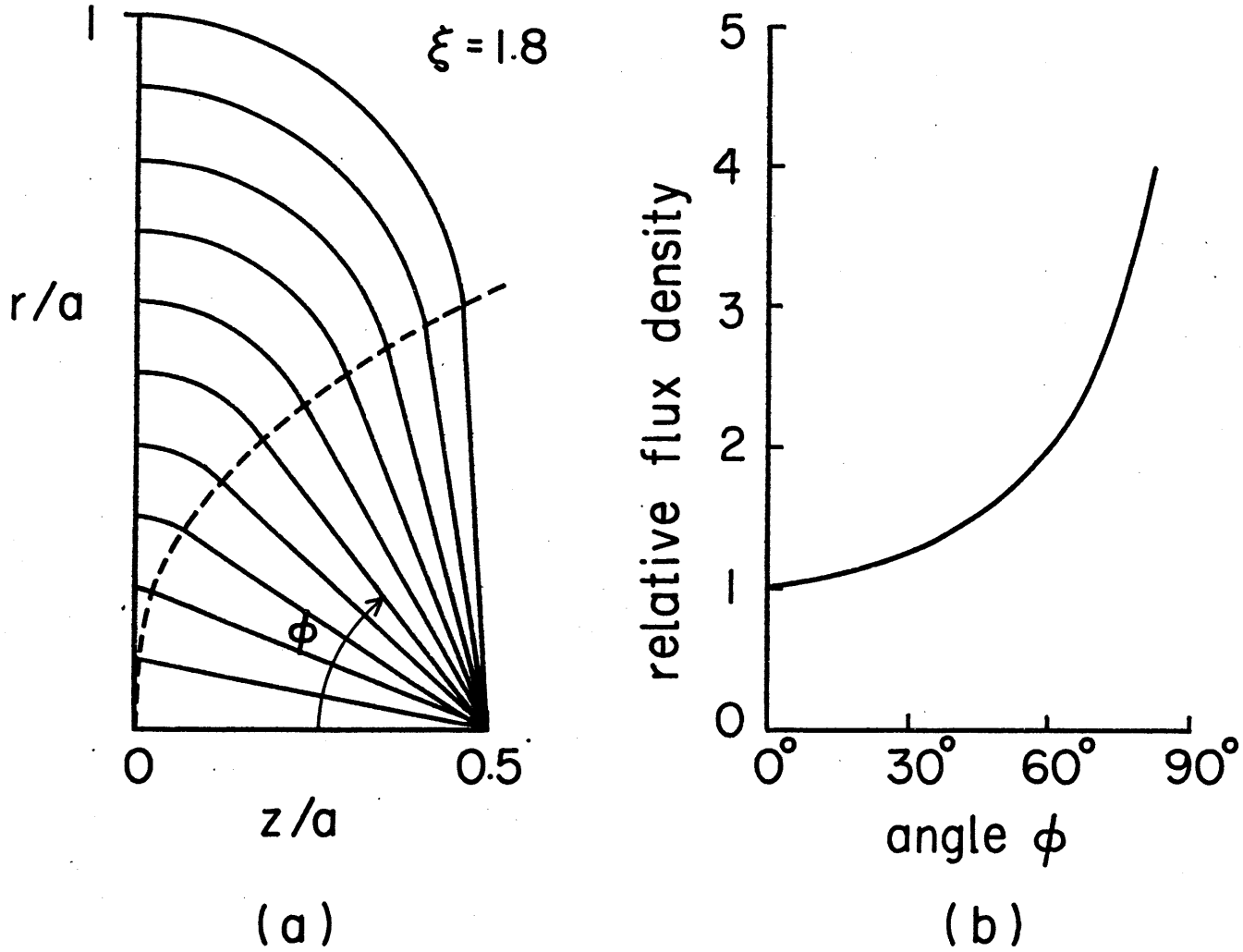
1
ξ = 1.8
r/a
0
0.5
z/a
φ
(a)
5
4
3
2
1
0
relative flux density
0°
30°
60°
90°
angle φ
(b)

FIG. 5

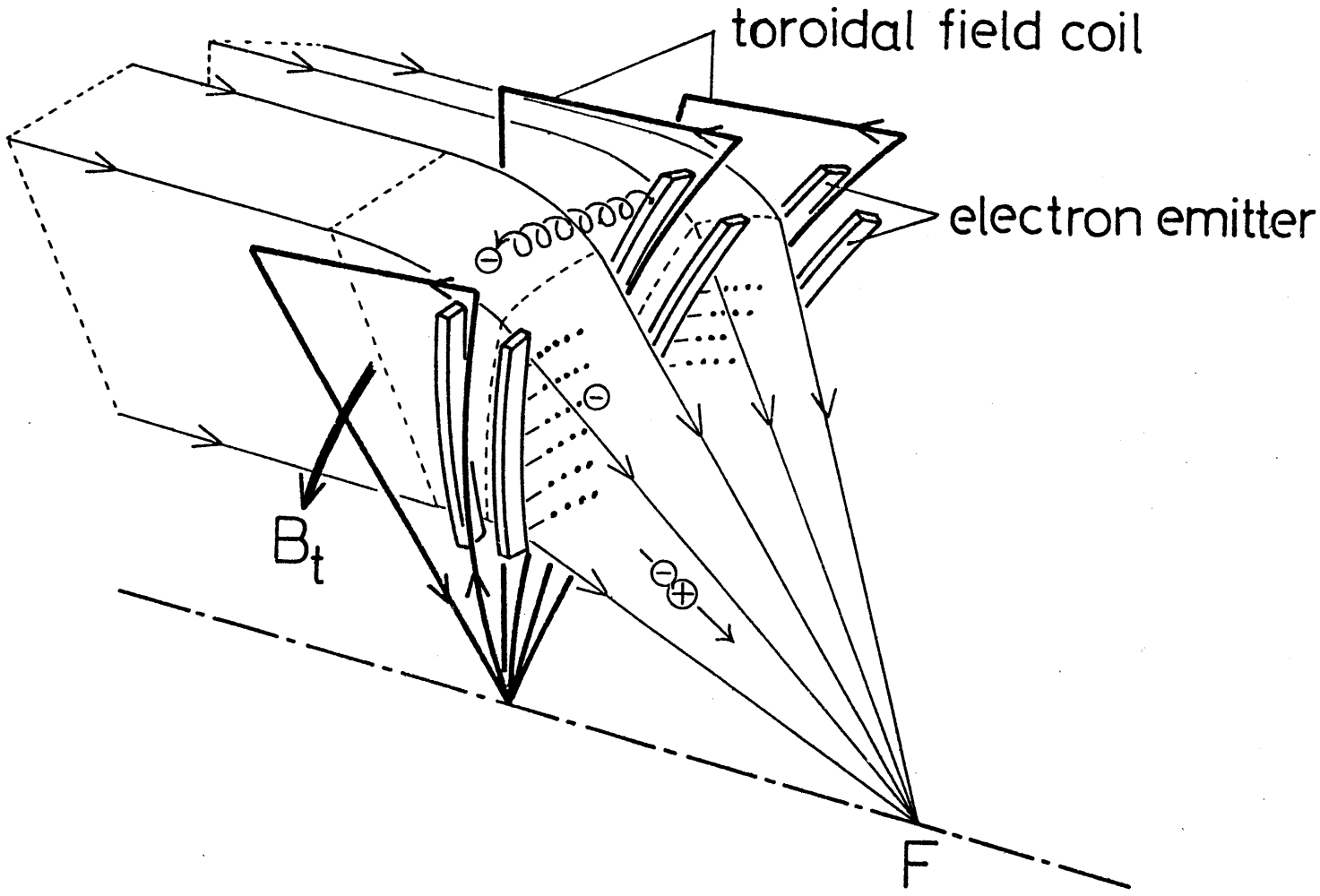

FIG. 6

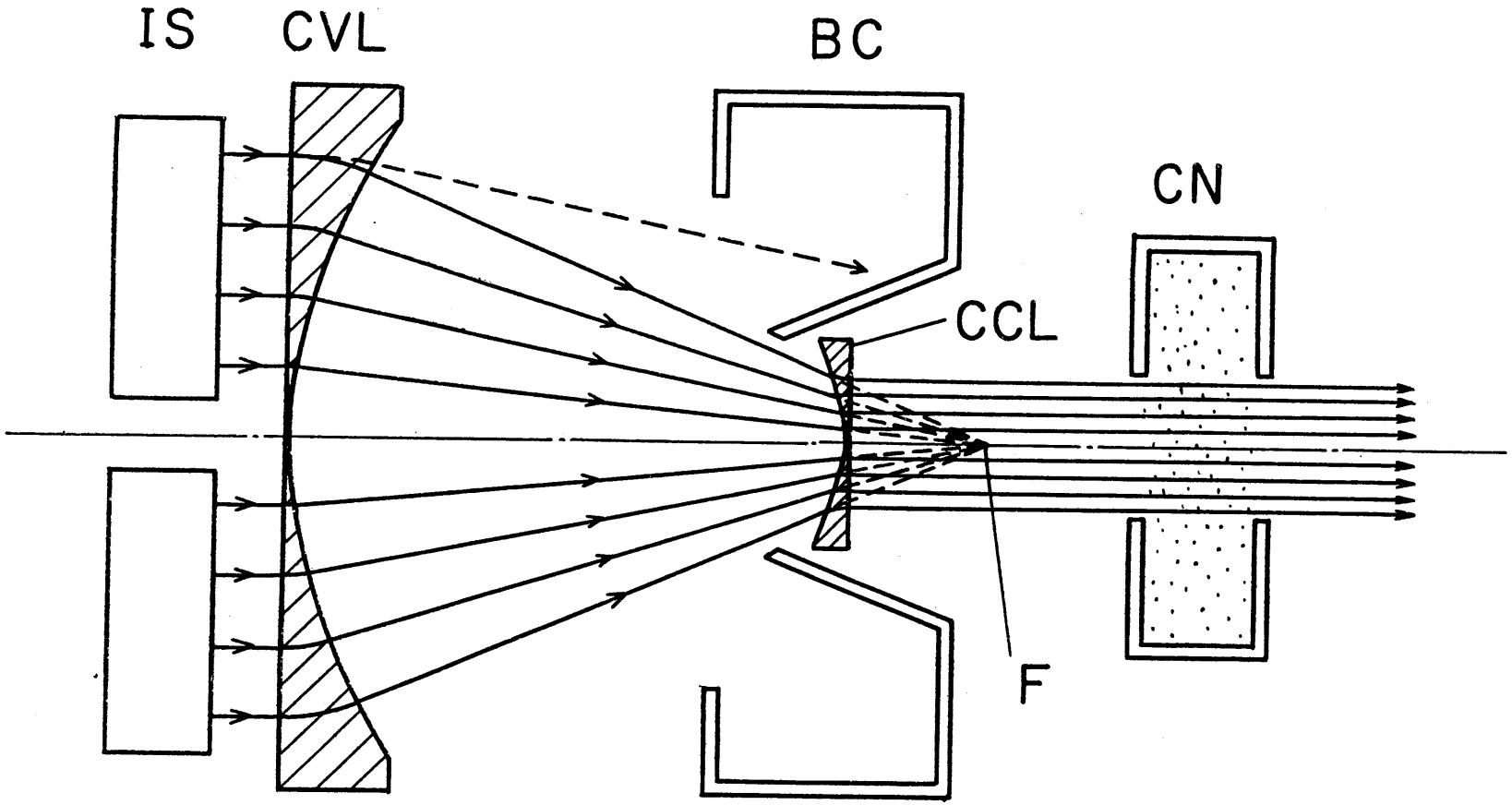

FIG. 7

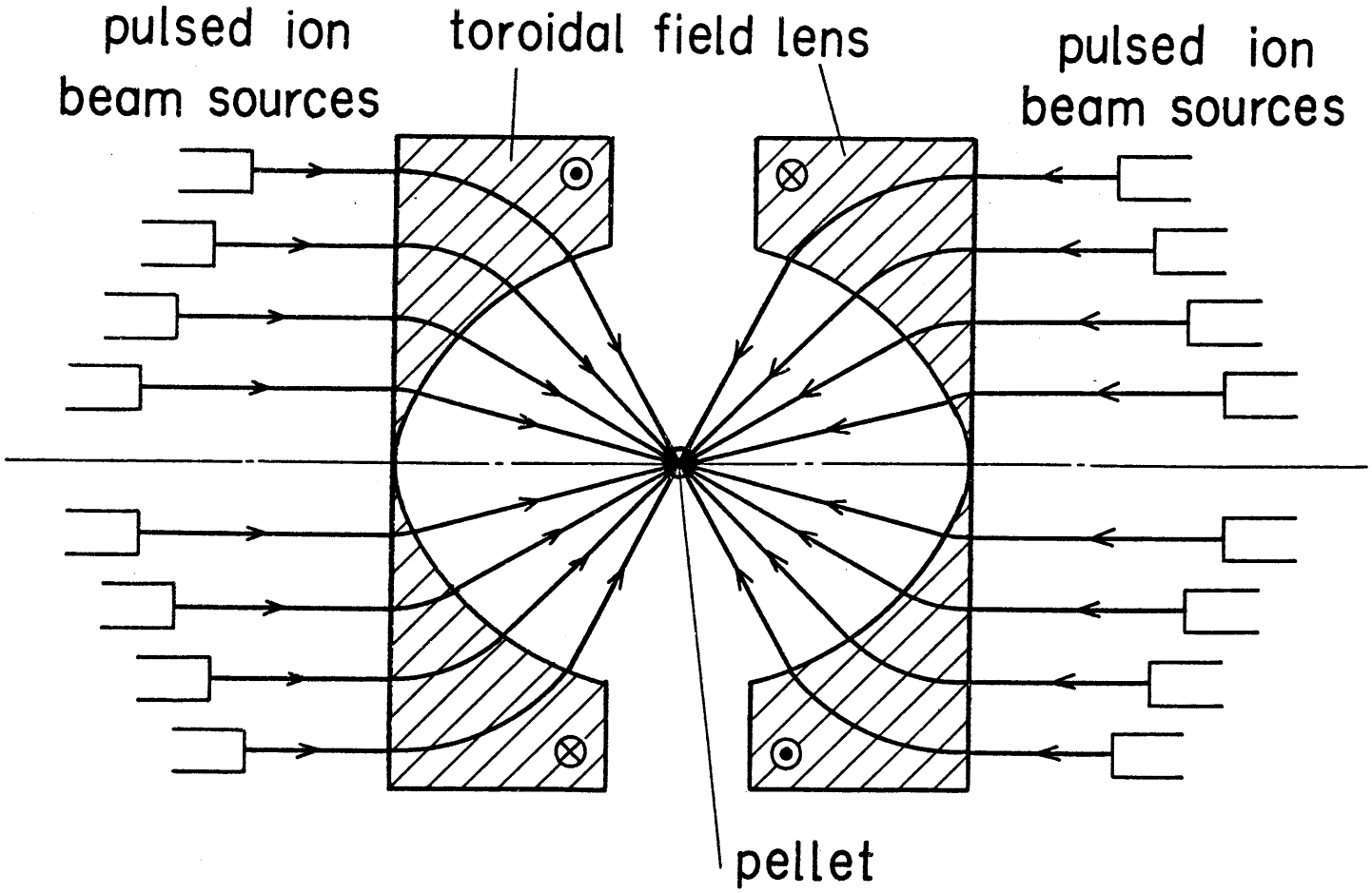
pulsed ion
beam sources
toroidal field lens
pulsed ion
beam sources
pellet

FIG. 8

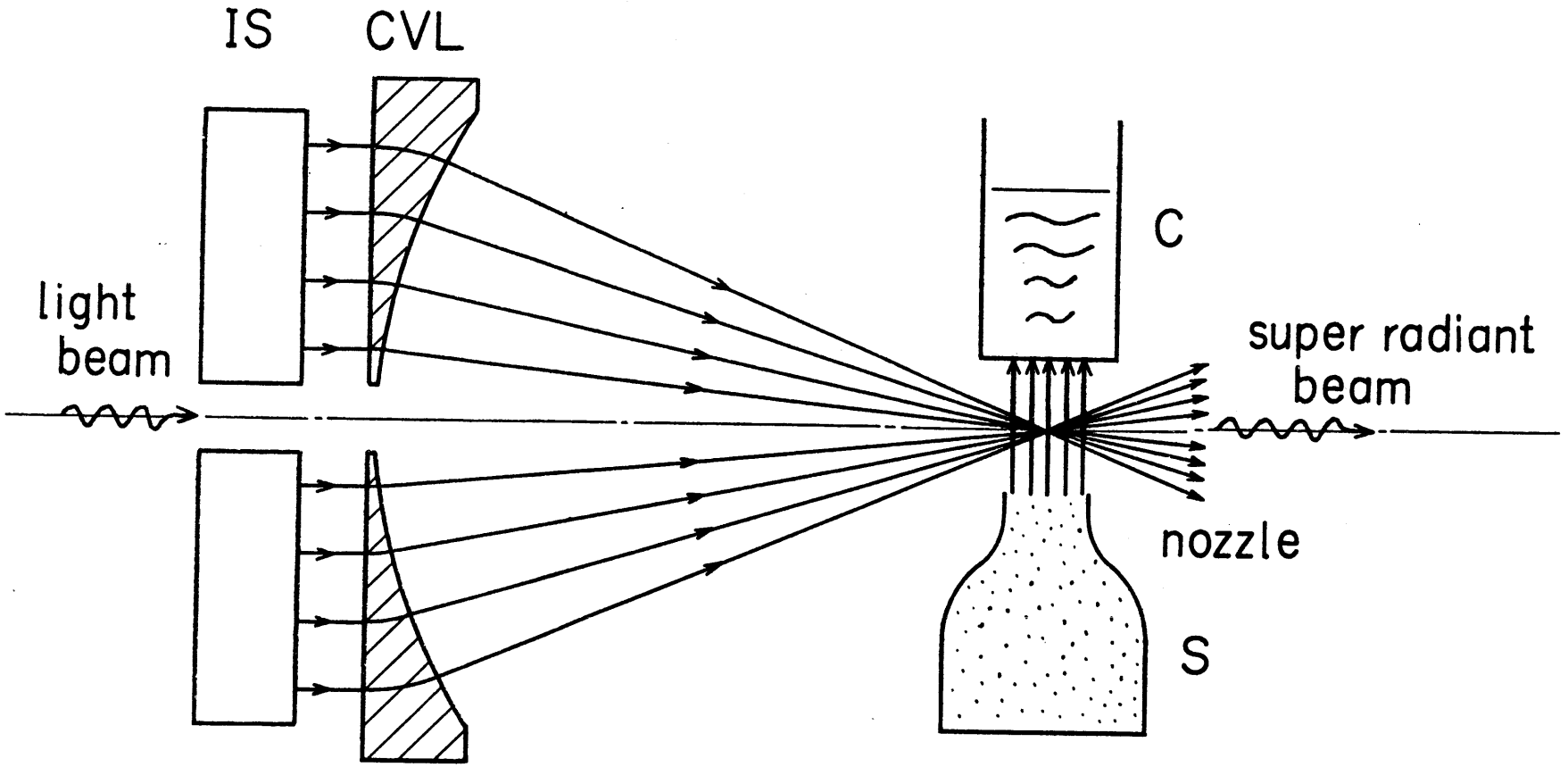

FIG. 9